Available online at www.sciencedirect.com

ScienceDirect

Mendeleev Commun., 2023, **33**, 212–214

Mendeleev Communications

Features of photoinduced proton transfer in the presence of a polyelectrolyte

Alina O. Naumova,[a] Pavel V. Melnikov,*[a] Vladimir A. Kuzmin[b] and Nikolay K. Zaitsev[a]

[a] *M. V. Lomonosov Institute of Fine Chemical Technologies, MIREA – Russian Technological University, 119571 Moscow, Russian Federation. E-mail: melnikovsoft@mail.ru*

[b] *N. M. Emanuel Institute of Biochemical Physics, Russian Academy of Sciences, 119334 Moscow, Russian Federation*

DOI: 10.1016/j.mencom.2023.02.020

Using the example of a series of sulfo derivatives of 2-naphthol, it was shown that the charge field formed by the polyelectrolyte coil significantly changes the constants k_1 and k_{-1} of the photoinduced proton transfer reaction, but no noticeable shift in the equilibrium constant K^* was found. This observation is fundamentally different from the behavior of these substances in micellar media, where K^* increases by an order of magnitude. The binding constants of the dyes with the cationic polyelectrolyte were also determined.

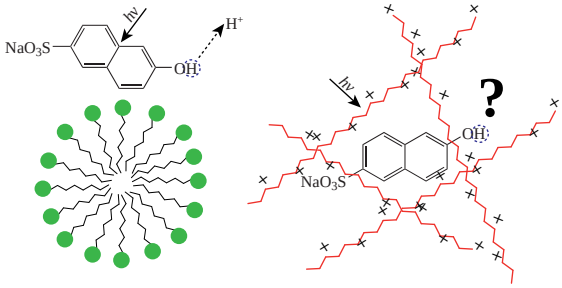

Keywords: fluorescence, photoacid, photoinduced proton transfer, acid–base reaction, excited state, shift in equilibrium, polyelectrolyte, 2-naphthol derivative.

Photoinduced proton transfer is obviously one of the most fundamental reactions in nature.[1] However, understanding how the environment mediates proton dynamics remains a fundamental challenge in chemistry and biochemistry and continues to be an area of active experimental and theoretical research.[2] Some compounds in the excited state become stronger acids (for example, hydroxy- and amino-substituted aromatic compounds); others, such as acridine or aromatic aldehydes, become stronger bases.[3–5]

Photochemical processes have been well studied in micelles[6–8] and liposomes,[9,10] but no systematic studies of this kind have been carried out in polyelectrolytes. One could assume that the process proceeds in the same way. However, the charge distribution of the polyelectrolyte differs from the charge distribution of micelles. Micelles of linear surfactants at the critical micelle concentration have a spherical shape, and the charge is distributed over the surface of the sphere.[11] Thus, a positive potential gradient is formed, which significantly accelerates the deprotonation reaction and shifts the equilibrium.[12] Polyelectrolytes, in turn, exist in the form of a Gaussian coil, where charged groups are evenly distributed along the polymer chains.[13]

This work is devoted to the study of the features of the photoprotolytic reaction in the field of a polyelectrolyte. A series of sulfo derivatives of 2-naphthol was chosen as a convenient model system, and polydiallyldimethylammonium chloride (PDDA) was used as a polyelectrolyte.† PDDA is known for its ability to adsorb well on the SiO_2 surface,[14,15] and it can be used to form hybrid structures using quantum dots[16] or to create optical sensors.[17] In both cases, the key factor is the Coulomb interaction between the charged centers of the polymer and the molecules. Optical sensors represent an important alternative to electrochemical methods,[18–20] and the study of organized media discussed in this work can expand both fundamental knowledge about the photoinduced proton transfer reaction and the possibility of its practical application.[21]

The Coulomb interaction of sulfo groups with a cationic polyelectrolyte leads to reversible binding,

$$\mathrm{ArOH} + n\mathrm{PDDA} \rightleftarrows \mathrm{ArOH}\cdot n\mathrm{PDDA},$$

characterized by the equilibrium constant K_{bind}:

$$K_{\mathrm{bind}} = [\mathrm{ArOH}\cdot n\mathrm{PDDA}]/[\mathrm{ArOH}]\,[\mathrm{PDDA}]^n. \quad (1)$$

The total number of dye molecules is constant:

$$[\mathrm{ArOH}] + [\mathrm{ArOH}\cdot n\mathrm{PDDA}] = \mathrm{const}. \quad (2)$$

Let us denote the fraction of bound molecules as $\alpha = [\mathrm{ArOH}\cdot n\mathrm{PDDA}]/\mathrm{const}$, then the fraction of unbound dye is $(1-\alpha) = [\mathrm{ArOH}]/\mathrm{const}$. Equation (1) gives:

$$K_{\mathrm{bind}}\,[\mathrm{PDDA}]^n = \alpha\,\mathrm{const}/[(1-\alpha)\mathrm{const}]\,. \quad (3)$$

Due to the electrostatic nature of the interaction, the binding of one dye molecule by PDDA does not affect the ability to bind subsequent molecules, *i.e.*, [PDDA] = const′. Thus, α can be found from equation (3) as:

$$\alpha = K_{\mathrm{bind}}\,[\mathrm{PDDA}]^n/\{1 + K_{\mathrm{bind}}\,[\mathrm{PDDA}]^n\}. \quad (4)$$

The fluorescence spectrum is a superposition of the emission of bound and unbound dye molecules:

$$I = I_\infty\,\alpha + I_{\mathrm{W}}\,(1-\alpha), \quad (5)$$

† Sodium salt of 2-naphthol-6-sulfonic acid **1**, disodium salt of 2-naphthol-3,6-disulfonic acid **2** and disodium salt of 2-naphthol-3,6,8-trisulfonic acid **3** (Vekton, Russia) were used in this work. PDDA solutions of the desired concentration were prepared from a 20% stock solution (Sigma-Aldrich, USA) by dilution with deionized water. The experiments were carried out in solutions with pH from 0 to 12.5 at a temperature of 25 ± 2 °C. For details, see Online Supplementary Materials.

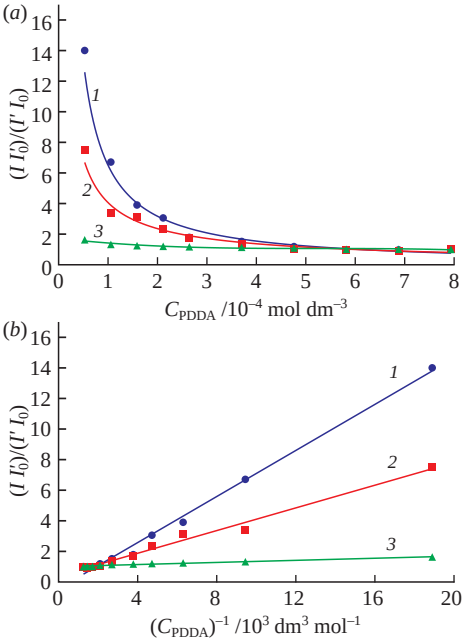

Figure 1 Dependence of the ratio of the fluorescence peak intensities of compounds (*1*) **1**, (*2*) **2** and (*3*) **3** on (*a*) the concentration of PDDA and (*b*) its reciprocal. $C_{Ind} = 4.7 \times 10^{-5}$ mol dm^{-3}.

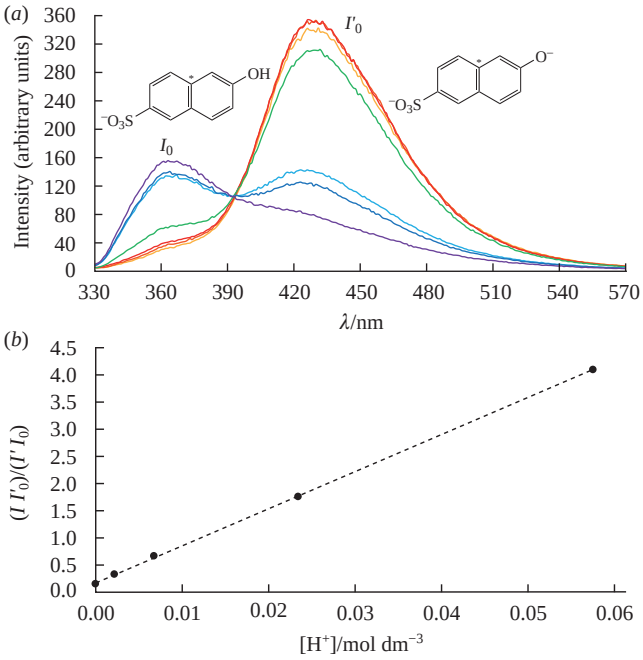

Figure 2 (*a*) pH dependence of the emission spectrum of compound **1** and (*b*) linearized plot of this dependence.

where I_∞ is the fluorescence intensity of ArOH molecules bound to PDDA, and I_W corresponds to unbound ArOH molecules in the aqueous phase. Substitution into equation (4) gives:

$$(I_\infty - I_W)/(I - I_W) = 1 + 1/\{K_{bind}\,[PDDA]^n\}. \quad (6)$$

The relative decrease in fluorescence intensity [Figure 1(*a*)] makes it possible to determine the concentration of PDDA at which almost all of the dye is bound. $C_{PDDA} = 5.8 \times 10^{-4}$ mol dm^{-3} was used in all further experiments with addition of polyelectrolyte. The concentration of the indicator in all experiments was 4.7×10^{-5} mol dm^{-3}. The straightening of the graph [Figure 1(*b*)] shows that the experimental dependences are linear with R^2 of 0.994, 0.987 and 0.981 over the entire range of PDDA concentrations for all the studied compounds, and the calculated K_{bind} are 1330, 2700 and 2900 dm^3 mol^{-1} for compounds **1**, **2** and **3**, respectively.

When a photoacid is excited to the S_1 state, referred to here as ArOH*, it becomes a much stronger proton donor. The processes are depicted in Scheme 1, which illustrates all relevant photophysics.[22] W is the excitation intensity, τ_0 and τ_0' are the lifetimes of the electronically excited molecules ArOH* and RO^{*-}, respectively, in the absence of protolytic reactions; $1/\tau_0$ and $1/\tau_0'$ are the decay rate constants of the excited states of the corresponding molecules. k_1 and k_{-1} are the rate constants of the forward and reverse reactions of deprotonation of the indicator in the excited state, characterized by the equilibrium constant $K^* = k_1/k_{-1}$.

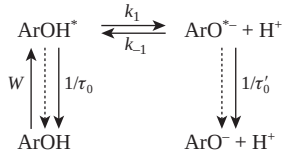

Scheme 1

The kinetic equations for electronically excited molecules have the form:

$$d[ArOH^*]/dt = W - (k_1 + 1/\tau_0)[ArOH^*] + k_{-1}[H^+][ArO^{*-}], \quad (7)$$

$$d[ArO^{*-}]/dt = k_1[ArOH^*] - \{k_{-1}[H^+] + 1/\tau_0'\}[ArO^{*-}]. \quad (8)$$

Under conditions of stationary photoexcitation, the concentrations of electronically excited molecules are constant:

$$d[ArOH^*]/dt = 0,\ d[ArO^{*-}]/dt = 0. \quad (9)$$

Under this condition, equation (8) takes the form:

$$[ArOH^*]/[ArO^{*-}] = k_{-1}[H^+]/k_1 + 1/\tau_0' k_1. \quad (10)$$

The concentrations of electronically excited molecules, up to constants, are proportional to the emission intensities in the corresponding bands of the fluorescence spectrum:

$$d[ArOH^*]/dt = I/\alpha,\ d[ArO^{*-}]/dt = I'/\beta. \quad (11)$$

Substituting equation (11) into (10) gives

$$(I\,I_0')/(I'\,I_0) = 1/k_1\tau_0 + k_{-1}\tau_0'[H^+]/k_1\tau_0\,. \quad (12)$$

If τ_0 and τ_0' are known, then, using equation (12), one can find the rate constants of the forward and reverse photoprotolytic reactions by measuring the fluorescence spectra at various proton concentrations. The spectra of compound **1** and the linearized plot are shown in Figure 2 . Similar dependences were obtained for compounds **2** and **3** (Figure S1, see Online Supplementary Materials).

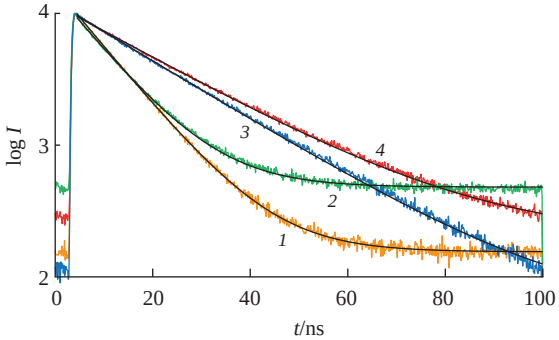

Figure 3 Fluorescence decay curves of the (*1*),(*2*) initial and (*3*),(*4*) deprotonated forms of compound **2** in the (*1*),(*3*) absence and (*2*),(*4*) presence of PDDA, recorded at λ of (*1*),(*2*) 364 and (*3*),(*4*) 430 nm. $C_{Ind} = 1.6 \times 10^{-6}$ mol dm^{-3}, $C_{PDDA} = 5.8 \times 10^{-4}$ mol dm^{-3}.

Table 1 Measured kinetic parameters[a] of sulfo derivatives of 2-naphthol in the absence and presence of PDDA ($C_{PDDA} = 5.8 \times 10^{-4}$ mol dm^{-3}).

Sample	τ_0/ns	τ_0'/ns	k_1/ns^{-1}	k_{-1}/ns^{-1}	K^*	pK^*
1	6.3	11.5	0.94	35.1	0.027	1.57
1 with PDDA	6.9	12.6	0.77	30.4	0.025	1.60
2	9.6	20.0	2.22	3.11	0.60	0.22
2 with PDDA	9.9	21.7	1.31	1.61	0.82	0.09
3	11.9	15.2	6.51	0.39	16.6	–1.22
3 with PDDA	12.0	17.8	1.17	0.09	13.3	–1.12
2N8S[b,c]		10.0	4.50	113	0.04	1.4
1N4S[b,d]					1.26	–0.1
1N-3,6diS[b,d]					398	–2.6

[a] Values determined with 10% uncertainty. [b] 2N8S: 2-naphthol-8-sulfonate; 1N-3,6diS: 1-naphthol-3,6-disulfonate; 1N4S: 1-naphthol-4-sulfonate, [c] Ref. 23. [d] Ref. 24.

The lifetimes of the initial (τ_0) and deprotonated (τ_0') forms for the systems under investigation were found experimentally from the fluorescence decay curves. Figure 3 shows the experimental data for compound **2** in the absence and presence of the polyelectrolyte with superimposed model monoexponential decay curves. Similar processing was carried out for compounds **1** and **3**, and the results are presented in Table 1. It can be seen that the lifetime of the deprotonated form significantly exceeds the lifetime of the initial form. The addition of PDDA has practically no effect on the lifetime of the initial form, but significantly increases the lifetime of the deprotonated form, which may be due to the effect of the field formed by the polyelectrolyte on the anion formed after proton detachment.

The found lifetimes make it possible to determine the kinetic parameters k_1 and k_{-1} of the deprotonation reaction (see Table 1). The addition of the cationic polyelectrolyte to the system leads to a significant shift in the rate constants of both the forward and reverse reactions. The shift naturally growths with an increase in the number of sulfo substituents in the molecule, as in the case of the reaction of the molecule in the ground state.[25] However, the change in k_1 and k_{-1} occurs symbatically, and as a result, the apparent equilibrium constant (K^*) changes slightly.

Thus, despite the obvious influence of the charge field formed by the polyelectrolyte on the activity coefficients, there is no noticeable shift in the equilibrium in the excited state, in contrast to the reaction in the ground state. This observation is fundamentally different from the behavior of these substances in micellar media, where the formed potential gradient leads to a preferential acceleration of the deprotonation reaction, that is, k_1, leading to a shift in the equilibrium constant K^* by an order of magnitude or more.[26]

This work was performed on the equipment of the Shared Science and Training Center for Collective Use of RTU MIREA with the support of the Ministry of Science and Higher Education of the Russian Federation (grant no. 075-15-2021-689, unique identification no. 2296.61321X0010). Spectral measurements were carried out at the Core Facility 'New Materials and Technologies' of the Institute of Biochemical Physics of RAS.

Online Supplementary Materials

Supplementary data associated with this article can be found in the online version at doi: 10.1016/j.mencom.2023.02.020.

References

1 J. R. Lakowicz, *Principles of Fluorescence Spectroscopy*, 3rd edn., Springer, New York, 2006.
2 P.-T. Chou and K. M. Solntsev, *J. Phys. Chem. B*, 2015, **119**, 2089.
3 Y. Li, X. Feng, A. Wang, Y. Yang, J. Fei, B. Sun, Y. Jia and J. Li, *Angew. Chem., Int. Ed.*, 2019, **58**, 796.
4 A. Das, S. Ayad and K. Hanson, *Org. Lett.*, 2016, **18**, 5416.
5 I. D. Sorokin, O. I. Gromov, V. I. Pergushov, D. A. Pomogailo and M. Ya. Melnikov, *Mendeleev Commun.*, 2020, **30**, 67.
6 C. Lawler and M. D. Fayer, *J. Phys. Chem. B*, 2015, **119**, 6024.
7 N. Chattopadhyay, R. Dutta and M. Chowdhury, *J. Photochem. Photobiol., A*, 1989, **47**, 249.
8 A. O. Naumova, A. K. Afanasyev, P. V. Melnikov and N. K. Zaitsev, *Mendeleev Commun.*, 2021, **31**, 833.
9 S. Chaudhuri, K. Basu, B. Sengupta, A. Banerjee and P. K. Sengupta, *Luminescence*, 2008, **23**, 397.
10 T. Kroetz, M. C. dos Santos, R. Beal, G. Modernell Zanotto, F. S. Santos, F. C. Giacomelli, P. F. B. Gonçalves, V. R. de Lima, A. G. Dal-Bó and F. S. Rodembusch, *Photochem. Photobiol. Sci.*, 2019, **18**, 1171.
11 Y. Wang, K. Kimura, P. L. Dubin and W. Jaeger, *Macromolecules*, 2000, **33**, 3324.
12 S. Abou-Al Einin, A. K. Zaitsev, N. K. Zaitsev and M. G. Kuzmin, *J. Photochem. Photobiol., A*, 1988, **41**, 365.
13 M. Muthukumar, *Macromolecules*, 2017, **50**, 9528.
14 J. Huang, X. Liu and E. Thormann, *Langmuir*, 2018, **34**, 7264.
15 I. W. Mwangi, J. C. Ngila, P. Ndungu and T. A. M. Msagati, *Water, Air, Soil Pollut.*, 2013, **224**, 1638.
16 O. V. Ovchinnikov, M. S. Smirnov, I. G. Grevtseva, V. N. Derepko, T. A. Chevychelova, L. Yu. Leonova, A. S. Perepelitsa and T. S. Kondratenko, *Kondensirovannye sredy i mezhfaznye granitsy* (*Condensed Matter and Interphases*), 2021, **23**, 49.
17 A. O. Naumova, P. V. Melnikov, E. V. Dolganova, N. A. Yashtulov and N. K. Zaitsev, *Tonkie Khim. Tekhnol.* (*Fine Chem. Technol.*), 2020, **15**(4), 59.
18 S. S. Kamanin, V. A. Arlyapov, T. V. Rogova and A. N. Reshetilov, *Appl. Biochem. Microbiol.*, 2014, **50**, 835 (*Biotekhnologiya*, 2014, no. 2, 80).
19 A. S. Kharkova, V. A. Arlyapov, A. D. Turovskaya, A. N. Avtukh, I. P. Starodumova and A. N. Reshetilov, *Appl. Biochem. Microbiol.*, 2019, **55**, 189 (*Prikl. Biokhim. Mikrobiol.*, 2019, **55**, 199).
20 S. S. Kamanin, V. A. Arlyapov, A. V. Machulin, V. A. Alferov and A. N. Reshetilov, *Russ. J. Appl. Chem.*, 2015, **88**, 463 (*Zh. Prikl. Khim.*, 2015, **88**, 458).
21 O. S. Wolfbeis, *BioEssays*, 2015, **37**, 921.
22 S. Green, T. Xiang, K. P. Johnston and M. A. Fox, *J. Phys. Chem.*, 1995, **99**, 13787.
23 O. Gajst, L. Pinto da Silva, J. C. G. Esteves da Silva and D. Huppert, *J. Phys. Chem. A.*, 2018, **122**, 6166.
24 M. Prémont-Schwarz, T. Barak, D. Pines, E. T. J. Nibbering and E. Pines, *J. Phys. Chem. B*, 2013, **117**, 4594.
25 A. O. Naumova, A. S. Mugabutaeva, P. V. Melnikov and N. K. Zaitsev, *Moscow Univ. Chem. Bull.*, 2021, **76**, 14.
26 M. Luiz, M. A. Biasutti and N. A. García, *Redox Rep.*, 2004, **9**, 199.

Received: 21st July 2022; Com. 22/6967